ELSEVIER

Tectonophysics 330 (2001) 45–68

TECTONOPHYSICS

www.elsevier.com/locate/tecto

Test and application of the time- and magnitude predictable-model to the intermediate and deep focus earthquakes in the subduction zones of the circum-Pacific belt

E.E. Papadimitriou*, C.B. Papazachos, T.M. Tsapanos

Department of Geophysics, University of Thessaloniki, P.O. Box 352-1, GR54006 Thessaloniki, Greece

Received 18 April 2000; accepted 29 September 2000

Abstract

The test and application of the time and magnitude predictable model in the subduction zones around the circum-Pacific belt is performed. Each subduction zone was separated in several seismogenic regions on the basis of tectonic and geometrical features of the subducting lithosphere and for three different depth ranges. The data derived from these seismogenic regions were used in order to check the suitability of the regional time and magnitude predictable model, as this model was defined for shallow events. The results obtained in the present study confirm that this model appropriately describes the behavior of deep seismicity in these regions, since a positive ($\bar{c} = 0.31 \pm 0.003$) and a negative ($\bar{C} = -0.13 \pm 0.047$) dependence were found for the logarithm of the interevent times and the magnitude of following mainshock, respectively, on the magnitude of the preceding mainshock. Moreover, the slip-predictable model was rejected, since a negative dependence was found ($\bar{E} = -0.19$) between the interevent times and the magnitudes of the following mainshock. Probabilities of occurrence of the future strong ($M \geq 7.0$) events in each seismogenic region have been determined for the next decade conditioned on the previous occurrence of such events. The magnitudes of the expected events have also been estimated. Statistical tests for the estimated probabilities exhibit a good correlation with the occurrence rate of such events. Furthermore, the statistical significance of the model has been studied through additional tests. The results of this study demonstrate the validity of the regional time and magnitude predictable model in the areas examined. © 2001 Elsevier Science B.V. All rights reserved.

Keywords: time- and magnitude-predictable model; Subduction zones; Circum-Pacific belt; conditional probabilities; statistical significance

1. Introduction

In late 1980s, it became evident that theoretical time- and/or magnitude-earthquake predictable models could be tested with real data and possibly be efficiently applied for intermediate-term prediction. Papazachos (1989) introduced one of the main methodologies concerning the time-dependent behavior of the seismic activity. This method is based on the concept of the time predictable model, originally proposed by Shimazaki and Nakata (1980). According to this model, the time interval between two large earthquakes is proportional to the slip of the preceding earthquake, that is, large earthquakes occur when the stress has reached a fixed upper limit. This model was found suitable to describe the seismicity behavior in several cases (Bufe et al., 1977; Shimazaki

* Corresponding author.
E-mail addresses: ritsa@geo.auth.gr (E.E. Papadimitriou), costas@lemnos.geo.auth.gr (C.B. Papazachos), tsapanops@geo.auth.gr (T.M. Tsapanos).

PII: S0040-1951(00)00218-3

and Nakata, 1980; Sykes and Quittmeyer, 1981), although some studies questioned the applicability of such kind of models (Davis et al., 1989; Kagan and Jackson, 1991a).

The regional time and magnitude predictable model was introduced by Papazachos (1989, 1992) and further developed by Papazachos and Papaioannou (1993). This model was initially applied in seismogenic regions of the Aegean and the surrounding area and exhibits two major differences from the time-predictable model, proposed by Shimazaki and Nakata (1980): (a) The model is applicable to broad seismogenic regions and not only to a single fault or a simple plate boundary; and (b) The time of the next mainshock is not usually proportional to the slip of the preceding mainshock. On the contrary, a general anticorrelation is usually observed since large events (large slip, large time interval to the next event) are usually followed by relatively smaller events. It is clear that these differences extend the applicability of the simple time-predictable model and allow its use for practical purposes. This model has been tested in several parts of the continental fracture system (Karakaisis, 1994; Panagiotopoulos, 1995; Papadimitriou, 1994; Papadimitriou and Papazachos, 1994; Papazachos et al., 1997a,b).

Recently, Papazachos et al. (1994a,b; 1997a,b) determined two empirical relations expressing the regional time and magnitude predictable model by using a data sample for shallow mainshocks of the continental fracture system. The same authors discussed the properties of the model and showed, through statistical tests, its superiority in comparison with the classical time-independent model. The sample used concerned 274 seismogenic regions in sixteen areas of this system and consisted of 1811 data sets (T_t, M_{min}, M_p, M_f), where T_t is the interevent time, M_{min} is the minimum magnitude considered, M_p is the magnitude of the preceding event and M_f is the magnitude of the following event. Therefore, the estimation of the model parameters can be considered very reliable, since it is not based on a limited number of observations from a specific seismogenic region but on a large global data sample. The previously mentioned relations are given by:

$$\log T_t = bM_{min} + cM_p + d \log m_o + q \quad (1)$$

$$M_f = BM_{min} + CM_p + D \log m_o + m \quad (2)$$

where m_o is the annual moment rate, measured in dyn cm yr^{-1}, for each seismogenic region and constants q and m depend on the broader seismogenic province. For the continental fracture system, the parameters of Eqs. (1) and (2) take the values $b = 0.19$, $c = 0.33$, $d = -0.39$, $B = 0.73$, $C = -0.28$ and $D = 0.40$ (Papazachos et al., 1994a, 1997a).

Eqs. (1) and (2) represent the time- and magnitude-predictable models, respectively, since M_{min}, M_p and m_o can be used to determine the time interval and magnitude of the following event with magnitude larger than M_{min}. For these equations constants b, c, q, B and D are always positive while constants d, C, and m are negative. Moreover, it has been shown that Eq. (1) is more robust than Eq. (2). Most of the terms in Eqs. (1) and (2) are self-explanatory, e.g. the Gutenberg–Richter law implies that for the number N of events with $M > M_{min}$ it holds that $\log N \approx -b'M_{min}$. If T is the return period for an event with $M > M_{min}$, we have that $T \approx N^{-1}$, therefore $\log T \approx -\log N$ and by combining with the previous relation we find that $\log T \sim bM_{min}$, where b is a constant, which should always be positive.

The aim of the present study is to examine the applicability of the regional time- and magnitude-predictable model in the seismogenic regions that have been defined for the Wadati–Benioff zones of the circum-Pacific belt. The data sample from these regions is completely independent from the one used in the estimation of the parameters of relations (1) and (2). Moreover, the generation of deep focus earthquakes is believed to be the result of different processes compared to shallow earthquakes. Therefore, if the previous model is also appropriate for this independent and physically different data sample, then it can be considered that it has a global applicability not affected by the data type or the region where it applies. On the other hand, in most areas of the world there is not adequate information about earthquake recurrence, due to limited period of instrumental recording. Even in circum-Pacific belt where large earthquakes occur more frequently, there are certain segments of plate boundaries that have not experienced even a single seismic cycle. From this point of view, it is of paramount importance to develop a methodology that can make use not only of the interevent times of the maximum earthquakes generated by the main fault of a certain seismogenic region, but also of the interevent times of smaller earthquakes coming by secondary faults. This is the main principle where the regional time- and magnitude-predictable model is based. The model parameters are estimated by a large amount of data coming from several seismogenic regions and they have been found to hold globally (Papazachos and Papadimitriou, 1997). It is then possible to calculate the model probabilities in a seismogenic region even if only one interevent time of strong events (occurrence of two mainshocks) is available. In this case, it provides a powerful tool enabling time dependent seismic hazard evaluation, even in the cases when only few observations are available, by a simple optimization of parameters q and m in relations (1) and (2).

Although the origin of intermediate and deep focus earthquakes is probably not similar to the brittle fracture assumed for shallow earthquakes, it is reasonable to be attributed to a certain type of shear failure (Richter, 1958). Kostrov and Das (1988) discussed the origin of earthquakes at large depths and arrived to the conclusion that even in this case, the earthquake source is macroscopically equivalent to a fracture under certain assumptions. Since not only the shallow depth seismic activity but the intermediate and deep one also constitutes a major threat for along-boundary areas, therefore, it is of significant importance to estimate the probability of occurrence of large intermediate and deep focus events in specific regions and for a specified time interval. The results of this estimation are also given in the present paper, contributing in that way to the time dependent seismic hazard evaluation for the intermediate and deep activity.

Papazachos and Papadimitriou (1997) give a detailed statistical evaluation of the model's global applicability. They showed that the statistical significance of the model does not always satisfy very strict quantitative criteria (90% confidence limits) when examined for a single seismogenic region, mainly due to data errors, but tests for its global applicability resulted in very high statistical confidence limits. Moreover, application of the model to an independent data set exhibited that the results are also robust when different seismic zonation techniques are used.

2. Data used and estimation of seismicity parameters

The data used in the present study are taken from the catalog of Gutenberg and Richter (1954) for the period 1904–1952. In order to check the completeness of the catalog the occurrence rate for several magnitude thresholds is examined. Completeness thresholds were determined by the standard method of visual inspection of time/frequency plots, defining the completeness level for a magnitude threshold since the time when the data begin to follow a linear relationship. This catalog was found to be complete for events with $M \geq 7.0$ for the period 1897–1930 and for events with $M \geq 6.5$ for the period 1931–1952. The magnitudes reported in Abe (1981) were taken for these events. These magnitudes are m_B magnitudes, that is body-wave long-period magnitudes, as well as surface wave magnitudes. The catalog of Rothe (1969) was used as our data source for the period 1953–1963 which includes all the events with $M \geq 6.0$. For this period surface waves magnitudes are reported, and only for the larger ones m_B magnitudes were taken from Abe (1981). For the period 1964–1995 the ISC bulletins were used, which include m_b for almost all the large events, that is, short-period body-wave magnitudes equal to or larger than 5.0.

In order to obtain a homogeneous magnitude scale for the whole catalog, an attempt was made to find and use known relations to transform the different magnitude scales into the moment magnitude scale, M_w, as it is introduced by Hanks and Kanamori (1979). According to Heaton et al. (1986) it is possible to obtain m_B (long-period body-wave magnitude) and m_b (short-period body-wave magnitude) as a function of moment magnitude, using appropriate relationships between M_s and m_B (Abe and Kanamori, 1980), M_s and m_b (Noguchi and Abe, 1977), and m_B and m_b (Abe, 1981). All the m_b magnitudes available for the time period 1964–1995 were transformed to m_B, according to the formula proposed by Abe (1981):

$$m_B = 1.5m_b - 2.2 \tag{3}$$

Abe and Kanamori (1980), through the examination of Gutenberg and Richter's original worksheets,

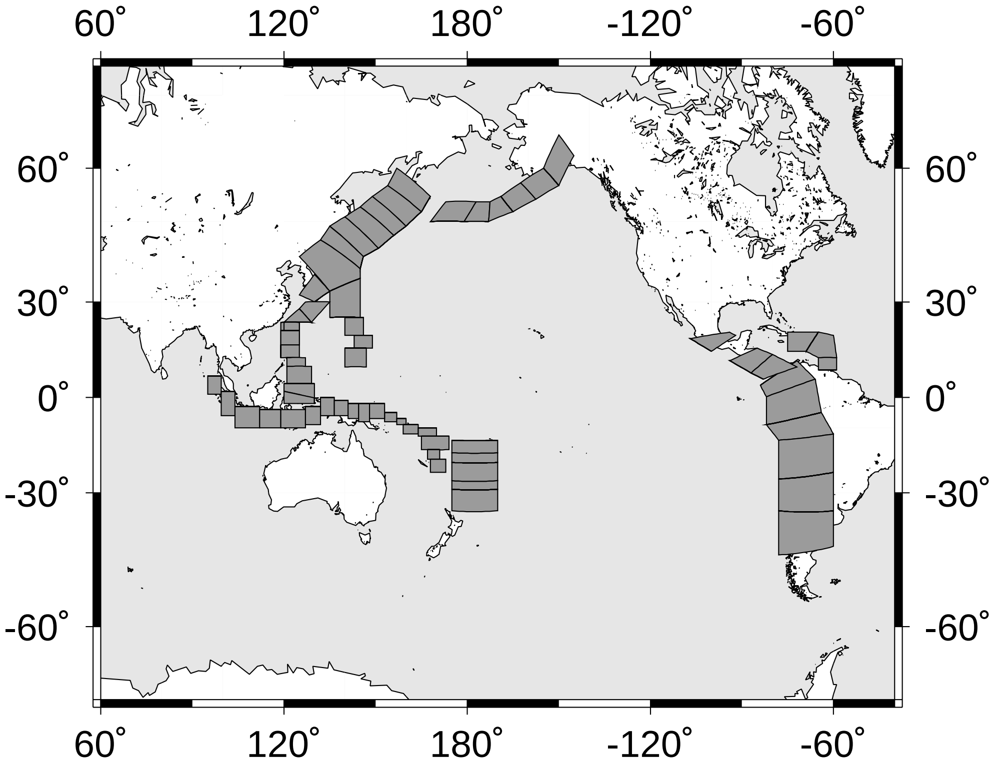

Fig. 1. Map of the seismogenic regions of deep seismicity examined in the present study.

found the following relation between m_B and M_s:

$$m_B = 0.65M_s + 2.5 \quad (4)$$

which satisfies the $m_B - M_s$ data for M_s between 5.2 and 8.7. Using this relation, all the available m_B magnitudes were transformed to M_s magnitudes. For those earthquakes, mainly during the period 1931–1963, for which only a general 'surface' magnitude was reported in the original catalogs, this magnitude was considered as M_s.

In the final step, all M_s-values were converted to M_w, considering that between $M_s = 6.0$ and $M_s = 8.0$, $M_s \cong M$. This is in agreement with Kanamori's (1977) earlier work. However, for magnitudes less than 6.0, M_s and M no longer coincide. For this reason, all the surface magnitudes above 6.0 were considered as moment magnitudes, while for the smaller ones the following relation was used:

$$M_w = 0.56M_s + 2.66 \qquad 5.0 \le M_s \le 6.0 \quad (5)$$

proposed by Papazachos et al. (1997c), which is almost identical with the corresponding curve given by Heaton et al. (1986). Through this procedure, a final catalog that includes a homogeneous moment magnitude scale was created. This catalog is complete and homogeneous for events with $M > 5.5$, $M > 6.0$, $M > 6.5$, and $M \ge 7.0$ for the periods 1966–1995, 1950–1995, 1930–1995 and 1897–1995, respectively.

The spatial distribution of the hypocenters of all the events included in the catalog was examined in order to define the separation of each subduction zone into several seismogenic regions. The procedure followed in order to define the seismogenic regions in each zone was based on the previously published information concerning map plots and cross-sections for indications of substantial lateral changes, offsets or tears of subduction zones and finally, together with the spatial distribution of volcanoes and trench bathymetry. Based on these

Table 1
Seismicity parameters (b', a, M_{max}, m_o (in dyn cm yr^{-1})) and expected strong mainshocks for each seismogenic region in the subduction zones of the circum-Pacific Belt. P_{10} is the probability for the occurrence of a mainshock with $M_s \geq 7.0$ during the period 1997–2006 and M_f is the most probable magnitude of the expected mainshock; the year of occurrence and the cumulative magnitude of each earthquake cluster (mainshock with its foreshocks and aftershocks in the broad sense) are given, respectively, in the last two columns

Region		Lat.	Long.	b'	a	M_{max}	log m_o	P_{10}	M_f	Year	M_{cum}
61–200 km											
SA-1	S. America	04.0	−84.0	1.10	6.23	7.5	26.97	0.61	7.7	1938	7.0
		12.0	−72.0							1957	6.8
		06.0	−66.0							1965	6.9
		00.2	−82.0							1973	7.2
										1979	7.5
										1995	7.4
SA-2		−09.0	−82.0	1.10	6.61	7.8	26.45	0.20	7.3	1937	7.3
		−05.0	−64.0							1950	7.1
		06.0	−66.0							1961	6.9
		00.2	−82.0							1965	7.2
										1971	7.5
										1983	7.9
										1995	7.8
SA-3		−09.0	−78.0	1.10	6.28	7.4	25.98	0.46	7.3	1932	6.8
		−05.0	−64.0							1946	7.0
		−12.0	−60.0							1957	6.5
		−14.0	−78.0							1963	7.1
										1974	7.5
										1984	6.6
										1991	7.2
SA-4		−26.0	−78.0	1.10	7.06	8.0	26.97	0.90	7.6	1940	7.6
		−24.0	−60.0							1950	8.2
		−12.0	−60.0							1964	6.8
		−14.0	−78.0							1967	7.8
										1976	8.1
										1991	7.5
SA-5		−26.0	−78.0	1.10	6.69	7.8	26.53	0.37	7.4	1932	6.9
		−24.0	−60.0							1939	7.5
		−35.0	−60.0							1956	7.1
		−35.0	−78.0							1965	7.7
										1980	7.0
										1985	7.6
										1993	7.8
SA-6		−35.0	−78.0	1.10	6.08	7.5	25.82	0.61	7.1	1934	7.4
		−35.0	−60.0							1949	7.1
		−44.0	−60.0							1962	7.5
		−46.0	−78.0								
MA-1	Mexico	19.0	−107.0	1.10	6.50	8.5	26.58	0.44	7.2	1937	7.4
		15.0	−100.0							1948	7.1
		20.0	−92.0							1964	7.4
		21.0	−94.0							1973	8.5
MA-2		12.0	−94.0	1.10	6.49	7.5	26.23	0.64	7.3	1937	6.5
		15.0	−100.0							1940	7.0
		20.0	−92.0							1946	7.3
		16.0	−85.0							1955	7.1
										1965	6.8
										1979	7.5
MA-3		12.0	−94.0	1.10	6.16	7.5	25.90	0.56	7.3	1947	6.9
		08.0	−87.0							1967	7.1
		14.0	−80.0							1982	7.2
		16.0	−85.0								
MA-4		06.0	−83.0	1.10	5.85	7.1	25.52	0.11	7.1	1939	6.5
		15.0	−100.0							1948	7.2

Table 1 (*continued*)

Region		Lat.	Long.	b'	a	M_{max}	log m_o	P_{10}	M_f	Year	M_{cum}
		20.0	−92.0							1992	7.1
		21.0	−94.0								
CA-1	Caribbean	15.0	−69.0	1.10	5.72	6.9	25.25	0.33	7.1	1935	6.5
		21.0	−65.0							1956	6.9
		21.0	−75.0							1979	7.0
		150	−75.0								
CA-2		15.0	−69.0	1.10	5.77	7.2	25.41	0.51	7.2	1953	7.1
		21.0	−65.0							1982	6.8
		20.0	−60.0								
		13.0	−59.0								
		13.0	−65.0								
CA-3		09.0	−65.0	1.10	5.50	7.1	25.90	0.67	7.5	1968	7.1
		09.0	−59.0							1983	6.5
		13.0	−59.0								
		13.0	−65.0								
NP-1	North Pacific	50.0	168.0	1.10	5.91	7.5	25.65	0.39	7.1	1940	7.5
		50.0	179.0							1958	6.6
		54.0	−177.0							1992	6.5
		54.0	173.0								
NP-2		50.0	−173.0	1.10	5.98	7.2	25.61	0.50	7.1	1933	6.7
		50.0	179.0							1937	7.2
		54.0	−177.0							1949	6.6
		54.0	172.5							1955	7.0
										1970	6.8
										1987	6.6
NP-3		55.0	−169.0	1.10	5.83	7.5	25.57	0.36	7.1	1946	6.7
		52.0	−165.0							1957	6.6
		50.0	−173.0								
		54.0	−172.5								
NP-4		55.0	−169.0	1.10	5.92	7.1	25.52	0.37	7.0	1944	7.2
		52.0	−165.0							1982	7.0
		54.5	−157.5								
		57.5	−162.5								
NP-5		60.0	−155.0	1.10	6.11	8.3	26.12	0.33	7.3	1941	6.5
		57.0	−150.0							1959	6.8
		54.5	−157.5							1979	6.5
		57.5	−162.5							1990	6.8
NP-6		60.0	−155.0	1.10	5.96	7.1	25.56	0.43	7.0	1934	7.2
		57.0	−150.0							1954	6.8
		62.0	−145.0							1968	6.5
		65.0	−150.0							1991	6.8
KK-1	Kuriles-Kamchhatka	42.0	146.0	1.10	6.75	8.7	26.89	0.88	7.8	1934	7.1
		44.0	151.0							1939	7.4
		51.0	140.0							1958	8.7
		49.0	135.0							1975	7.0
										1978	8.3
										1994	7.2
KK-2		44.0	151.0	1.10	6.39	7.5	26.13	0.21	7.4	1937	6.5
		47.0	156.0							1942	7.5
		53.0	145.0							1956	7.5
		51.0	140.0							1974	6.5
										1986	6.7
										1991	6.6
										1994	7.5
										1993	7.5
KK-3		47.0	156.0	1.10	6.32	7.5	26.06	0.64	7.6	1949	7.1

Table 1 (*continued*)

Region		Lat.	Long.	b'	a	M_{max}	log m_o	P_{10}	M_f	Year	M_{cum}
		49.0	160.0							1964	7.2
		55.0	149.0							1972	7.5
		53.0	145.0							1990	6.9
KK-4		49.0	160.0	1.10	6.38	7.5	26.12	0.25	7.4	1937	6.5
		52.0	165.0							1941	6.9
		57.0	154.0							1953	7.1
		55.0	149.0							1960	7.4
										1971	7.6
										1983	6.8
										1993	7.5
KK-5		52.0	165.0	1.10	5.92	8.0	25.83	0.17	7.2	1957	6.8
		55.0	168.0							1975	6.5
		60.0	157.0							1983	8.0
		57.0	154.0								
JP-1	Japan	30.0	130.0	1.10	6.13	7.7	25.93	0.33	7.3	1960	6.5
		33.0	135.0							1978	7.4
		37.5	130.0								
		32.0	125.0								
JP-2		33.0	135.0	1.10	6.42	7.5	26.16	0.35	7.4	1933	6.9
		36.5	145.0							1937	7.2
		39.0	145.0							1961	7.0
		46.0	132.0							1965	7.2
		42.0	125.0							1978	7.0
										1987	7.5
JP-3		39.0	145.0	1.10	6.52	8.6	26.63	0.18	7.3	1931	6.7
		42.0	146.0							1944	6.6
		49.0	135.0							1953	7.1
		46.0	132.0							1974	6.6
										1981	7.4
										1987	7.8
										1993	8.6
IBM-1	Izu Bonin-Marianas	25.5	135.0	1.10	6.46	8.0	26.37	0.55	7.4	1933	6.8
		25.5	145.0							1956	6.5
		36.5	145.0							1964	7.5
		33.0	135.0							1972	8.1
										1987	7.5
IBM-2		25.5	140.0	1.10	6.19	8.3	26.20	0.55	7.6	1932	6.5
		25.5	146.0							1957	7.2
		20.0	146.0							1982	6.5
		20.0	140.0								
IBM-3		20.0	143.0	1.10	6.22	7.4	25.92	0.52	7.4	1931	7.1
		20.0	149.0							1940	7.7
		16.0	149.0							1953	7.0
		16.0	143.0							1965	6.9
										1974	6.5
										1983	6.9
IBM-4		16.0	140.0	1.10	6.10	7.1	25.70	0.47	7.5	1942	7.1
		16.0	147.0							1950	7.1
		10.0	147.0							1961	6.5
		10.0	140.0							1967	7.0
										1984	6.5
RK-1	Ryukyu	24.0	129.0	1.10	6.32	8.6	26.43	0.67	7.4	1951	7.0
		28.0	125.0							1960	6.7
		30.0	127.0							1965	7.0
		30.0	135.0							1983	6.5
										1991	7.1

Table 1 (*continued*)

Region		Lat.	Long.	b'	a	M_{max}	log m_o	P_{10}	M_f	Year	M_{cum}
RK-2		24.0	120.0	1.10	5.87	7.8	25.71	0.47	7.2	1947	7.5
		24.0	129.0							1959	7.8
		28.0	125.0							1970	6.5
										1978	7.0
PH-3	Philippines	24.0	125.0	1.10	6.13	7.5	25.43	0.03	6.9	1930	7.2
		24.0	119.0							1959	6.9
		17.0	119.0							1965	7.1
		17.0	125.0							1983	6.8
										1993	7.5
PH-4		17.0	119.0	1.10	6.14	7.4	25.84	0.26	7.1	1940	6.9
		13.0	119.0							1959	7.0
		13.0	125.0							1985	7.6
		17.0	125..0								
PH-5		10.2	121.0	1.10	5.61	6.7	25.07	–	–	1942	6.7
		10.2	127.0							1980	6.6
		13.0	127.0								
		13.0	121.0								
PH-6		04.5	121.0	1.10	6.72	7.4	26.42	0.56	7.3	1932	6.7
		04.5	129.0							1936	7.1
		10.2	129.0							1945	6.7
		10.2	121.0							1949	7.5
										1965	7.2
										1972	7.7
										1984	6.5
										1987	7.5
PH-7		04.5	120.0	1.10	6.73	8.5	26.81	0.68	7.5	1940	6.7
		04.5	130.0							1948	7.2
		−00.2	130.0							1958	7.2
		02.0	120.0							1966	8.5
										1989	7.6
PH-8		−00.2	130.0	1.10	6.70	8.2	26.67	0.77	7.5	1932	6.8
		−02.0	130.0							1936	6.7
		−02.0	120.0							1939	8.2
		−02.0	120.0							1953	6.8
										1961	7.3
										1964	7.5
										1975	7.1
										1985	6.5
										1989	7.2
IND-1	Indonesia	07.0	95.0	1.10	6.21	8.2	26.18	0.59	7.5	1934	7.0
		07.0	99.5							1960	6.5
		01.0	99.5							1964	8.2
		01.0	95.0							1989	6.5
										1993	7.1
IND-2		02.0	99.5	1.10	6.35	7.4	26.05	0.52	7.5	1932	6.7
		02.0	104.0							1938	7.1
		−06.0	104.0							1943	7.1
		−06.0	99.5							1956	6.9
										1967	7.6
										1978	6.5
										1994	7.0
IND-3		−03.0	104.0	1.10	6.43	7.8	26.27	0.71	7.7	1943	7.8
		−03.0	112.0							1958	6.6
		−10.0	112.0							1965	7.5
		−10.0	104.0							1976	6.5
										1979	7.1
										1992	6.5
IND-4		−04.0	112.0	1.10	6.18	7.1	25.78	0.46	7.3	1938	6.5

Table 1 (*continued*)

Region		Lat.	Long.	b'	a	M_{max}	log m_o	P_{10}	M_f	Year	M_{cum}
		−04.0	119.0							1953	6.5
		−10.0	119.0							1957	6.9
		−10.0	112.0							1967	7.0
										1985	7.3
IND-5		−04.0	119.0	1.10	6.18	7.4	25.88	0.43	7.3	1938	7.2
		−04.0	127.0							1943	7.8
		−10.0	127.0							1957	7.0
		−10.0	119.0							1957	7.0
										1965	7.7
										1976	6.5
										1979	7.1
										1985	7.4
IND-6		−03.0	127.0	1.10	7.07	8.2	27.04	0.63	7.5	1931	7.3
		−03.0	132.0							1946	6.7
		−09.0	132.0							1931	7.3
		−09.0	127.0							1956	7.4
										1963	8.4
										1977	6.8
										1983	7.6
										1987	8.3
GU-1	New Guinea	−0.01	132.0	1.10	5.83	7.1	25.43	0.46	7.1	1937	7.0
		−0.01	136.5							1959	7.0
		−06.0	136.5							1978	7.1
		−06.0	132.0								
GU-2		−01.0	136.5	1.10	6.11	7.5	25.85	0.18	7.2	1955	7.0
		−01.0	141.0							1964	6.6
		−06.0	141.0							1968	6.8
		−06.0	136.5							1991	7.5
GU-3		−02.0	141.0	1.10	6.51	8.0	26.42	0.48	7.2	1936	7.2
		−02.0	144.5							1943	7.4
		−07.0	144.5							1961	7.1
		−07.0	141.0							1964	7.6
										1975	8.3
GU-4		−02.0	144.5	1.10	6.69	7.8	26.53	0.75	7.5	1934	7.3
		−02.0	148.0							1946	7.4
		−08.0	148.0							1951	7.5
		−08.0	144.5							1965	8.0
										1979	7.2
										1987	7.5
GU-5		−02.0	148.0	1.10	6.73	8.0	26.64	0.47	7.4	1937	7.0
		−02.0	153.0							1944	7.2
		−07.0	153.0							1956	6.5
		−07.0	148.0							1960	7.2
										1971	7.7
										1984	7.3
										1990	8.0
SH-1	Solomon Hebrides	−5.0	153.0	1.10	6.51	7.1	26.11	0.55	7.3	1934	7.1
		−05.0	157.0							1951	7.1
		−08.0	157.0							1955	7.1
		−08.0	153.0							1970	7.0
										1976	7.4
										1986	7.2
SH-2		−07.0	157.0	1.10	5.84	7.5	25.58	0.33	7.0	1969	7.5
		−07.0	160.0								
		−09.0	160.0								
		−09.0	157.0								
SH-3		−09.0	159.0	1.10	6.30	7.4	26.00	0.49	7.4	1937	7.2

Table 1 (*continued*)

Region		Lat.	Long.	b'	a	M_{max}	log m_o	P_{10}	M_f	Year	M_{cum}
		−09.0	164.0							1955	7.1
		−12.0	164.0							1973	7.6
		−12.0	159.0							1985	6.8
										1989	7.0
SH-4		−10.0	164.0	1.10	6.49	8.3	26.50	0.56	7.5	1942	7.0
		−10.0	170.0							1953	6.9
		−12.7	170.0							1957	7.3
		−12.7	164.0							1971	7.6
										1975	8.0
										1994	7.2
SH-5		−12.7	165.0	1.10	6.90	8.2	26.87	0.53	7.8	1935	7.4
		−12.7	174.0							1939	7.6
		−17.0	174.0							1951	7.4
		−17.0	165.0							1964	8.1
										1978	8.3
										1991	6.8
SH-6		−17.0	167.0	1.10	6.58	8.3	26.59	0.40	7.4	1934	6.7
		−17.0	171.0							1939	7.0
		−20.0	171.0							1944	7.7
		−20.0	167.0							1959	6.5
										1963	7.2
										1973	6.8
										1986	7.2
										1992	7.8
SH-7		−20.0	168.0	1.10	6.72	8.6	26.83	0.54	7.2	1931	7.1
		−20.0	173.0							1935	7.5
		−24.0	173.0							1944	7.5
		−24.0	168.0							1961	6.9
										1966	7.5
										1981	8.6
KER-1	Kermadec	−29.0	−170.0	1.10	6.18	7.3	25.85	0.74	7.5	1932	6.5
		−29.0	175.0							1941	6.9
		−26.5	175.0							1949	7.2
		−26.5	−170.0							1959	7.4
										1972	7.1
										1987	6.8
KER-2		−29.0	−170.0	1.10	6.37	7.5	26.11	0.57	7.5	1937	6.8
		−29.0	175.0							1943	7.2
		−35.0	175.0							1957	7.3
		−35.0	−170.0							1970	6.8
										1976	7.6
										1987	6.5
										1990	7.1
TNG-1	Tonga	−14.0	−170.0	1.10	6.47	7.8	26.31	0.36	7.3	1939	7.1
		−14.0	175.0							1955	7.2
		−18.0	175.0							1968	6.9
		−18.0	−170.0							1984	8.1
TNG-2		−21.0	−170.0	1.10	6.27	8.0	26.18	0.64	7.4	1950	7.8
		−21.0	175.0							1982	6.5
		−18.0	175.0							1988	7.3
		−18.0	−170.0								
TNG-3		−21.0	−170.0	1.10	6.72	8.5	26.80	0.69	7.7	1933	6.5
		−21.0	175.0							1940	6.7
		−26.5	175.0							1943	7.3
		−26.5	−170.0							1954	7.2
										1965	6.9
										1970	7.8
										1977	8.6

Table 1 (*continued*)

Region		Lat.	Long.	b'	a	M_{max}	log m_o	P_{10}	M_f	Year	M_{cum}
										1995	7.4
201–400 Km											
SA-4	S. America	−26.0	−78.0	0.90	5.06	8.0	26.37	0.04	7.2	1933	6.9
		−24.0	−60.0							1941	7.4
		−12.0	−60.0							1952	7.3
		−14.0	−78.0							1973	6.9
										1987	6.9
										1993	8.0
KK-1	Kuriles-Kamchatka	42.0	146.0	0.90	4.82	7.7	25.96	0.64	7.7	1933	7.1
		44.0	151.0							1950	7.7
		51.0	140.0							1969	7.5
		49.0	135.0							1985	6.7
KK-2		47.0	156.0	0.90	4.11	6.5	24.73	–	–	1957	6.5
		49.0	160.0							1984	6.6
		55.0	149.0								
		53.0	145.0								
KK-3		47.0	156.0	0.90	4.11	6.5	24.61	–	–	1931	6.5
		49.0	160.0								
		55.0	149.0								
		53.0	145.0								
KK-4		49.0	160.0	0.90	4.61	7.5	25.65	–	–	1934	6.9
		52.0	165.0								
		57.0	154.0								
		55.0	149.0								
JP-2	Japan	33.0	135.0	0.90	4.83	7.5	25.87	0.26	7.1	1931	7.5
		36.5	145.0							1942	6.5
		39.0	145.0							1954	6.8
		46.0	132.0							1967	6.8
		42.0	125.0							1995	6.6
JP-3		39.0	145.0	0.90	4.71	7.5	25.75	0.25	7.1	1932	7.3
		42.0	146.0							1963	6.7
		49.0	135.0							1981	6.6
		46.0	132.0								
IBM-1	Izu Bonin-Marianas	25.5	135.0	0.90	5.04	8.0	26.35	0.32	7.2	1943	6.8
		25.5	145.0							1964	7.8
		36.5	145.0							1978	6.8
		33.0	135.0							1984	7.9
IBM-2		25.5	140.0	0.90	4.66	7.5	25.70	0.02	7.1	1932	6.8
		25.5	146.0							1948	6.7
		20.0	146.0							1965	6.6
		20.0	140.0							1969	6.8
										1995	7.5
IBM-3		20.0	143.0	0.90	4.50	6.9	25.21	–	–	1934	6.5
		20.0	149.0							1956	6.9
		16.0	149.0							1979	6.5
		16.0	143.0								
RK-1	Ryukyu	24.0	129.0	0.90	4.44	6.8	25.10	–	–	1936	6.5
		28.0	125.0							1953	6.9
		30.0	127.0							1981	6.8
		30.0	135.0								
PH-6	Philippines	04.5	121.0	0.90	4.57	7.5	25.61	0.28	7.2	1984	7.5
		04.5	129.0								
		10.2	129.0								
		10.2	121.0								

Table 1 (*continued*)

Region		Lat.	Long.	b'	a	M_{max}	log m_o	P_{10}	M_f	Year	M_{cum}
PH-7		04.5	120.0	0.90	4.59	6.5	25.09	–	–	1932	6.5
		04.5	130.0								
		−00.2	130.0								
		02.0	120.0								
PH-8		−00.2	130.0	0.90	4.36	7.1	25.18	0.24	7.1	1955	6.6
		−02.0	130.0							1984	7.1
		−02.0	120.0								
		02.0	120.0								
IND-3	Indonesia	−03.0	104.0	0.90	4.34	7.8	25.54	0.98	7.2	1943	7.8
		−03.0	112.0							1958	6.6
		−10.0	112.0							1965	7.5
		−10.0	104.0							1976	6.5
										1979	7.1
										1992	6.5
IND-4		−04.0	112.0	0.90	4.24	6.5	24.74	–	–	1938	6.5
		−04.0	119.0							1953	6.5
		−10.0	119.0							1957	6.9
		−10.0	112.0							1967	7.0
										1985	7.3
IND-5		−04.0	119.0	0.90	4.61	8.0	25.92	0.99	7.3	1938	7.2
		−04.0	127.0							1943	7.8
		−10.0	127.0							1957	7.0
		−10.0	119.0							1957	7.0
IND-6		−03.0	127.0	0.90	4.61	7.5	25.65	0.99	7.4	1941	6.7
		−03.0	132.0							1950	7.5
		−09.0	132.0							1965	7.1
		−09.0	127.0								
GU-4	New Guinea	−02.0	144.5	0.90	4.49	6.6	25.04	–	–	1981	6.9
		−02.0	148.0							1992	6.6
		−08.0	148.0								
		−08.0	144.5								
GU-5		−02.0	148.0	0.90	4.34	7.1	25.16	0.47	7.1	1932	6.5
		−02.0	153.0							1938	6.7
		−07.0	153.0							1956	7.1
		−07.0	148.0								
SH-1	Solomon Hebrides	−05.0	153.0	0.90	4.33	7.2	25.20	0.46	7.2	1932	7.2
		−05.0	157.0							1964	6.6
		−08.0	157.0								
		−08.0	153.0								
SH-4		−10.0	164.0	0.90	4.49	6.8	25.15	–	–	1955	6.8
		−10.0	170.0							1966	6.9
		−12.7	170.0							1986	6.5
		−12.7	164.0								
SH-5		−12.7	165.0	0.90	4.96	7.4	25.94	0.24	7.3	1938	6.5
		−12.7	174.0							1946	6.7
		−17.0	174.0							1960	7.2
		−17.0	165.0							1973	6.8
										1978	7.4
										1992	7.4
SH-6		−17.0	167.0	0.90	4.87	7.8	26.07	0.18	7.3	1939	6.5
		−17.0	171.0							1943	6.8
		−20.0	171.0							1953	7.4
		−20.0	167.0							1970	7.4
										1994	7.5
KER-1	Kermadec	−29.0	−170.0	0.90	4.24	7.2	25.11	0.30	6.8	1950	7.2
		−29.0	175.0								

Table 1 (*continued*)

Region		Lat.	Long.	b'	a	M_{max}	log m_o	P_{10}	M_f	Year	M_{cum}
		−26.5	175.0								
		−26.5	−170.0								
KER-2		−29.0	−170.0	0.90	4.81	6.6	25.36	–	–	1951	6.8
		−29.0	175.0							1981	6.9
		−35.0	175.0							1994	6.6
		−35.0	−170.0								
TNG-1	Tonga	−14.0	−170.0	0.90	4.90	7.5	25.94	0.25	7.1	1935	7.1
		−14.0	175.0							1951	7.0
		−18.0	175.0							1972	7.2
		−18.0	−170.0							1984	6.8
										1989	7.5
TNG-2		−21.0	−170.0	0.90	5.06	8.0	26.37	0.66	7.3	1934	6.5
		−21.0	175.0							1946	7.2
		−18.0	175.0							1962	6.9
		−18.0	−170.0							1980	6.6
										1970	6.1
										1986	7.2
TNG-3		−21.0	−170.0	0.90	4.93	7.7	26.07	0.41	7.3	1937	7.7
		−21.0	175.0							1954	7.1
		−26.5	175.0							1969	6.5
		−26.5	−170.0							1975	7.2
										1979	7.5
										1992	7.1
$h > 400$ km											
SA-2	S. America	−09.0	−82.0	1.10	6.15	7.7	25.95	0.40	7.3	1970	7.7
		−05.0	−64.0								
		06.0	−66.0								
		00.2	−82.0								
SA-3		−09.0	−82.0	1.10	6.15	7.7	26.41	0.27	7.3	1935	7.0
		−05.0	−64.0							1950	7.2
		−12.0	−60.0							1961	7.7
		−14.0	−78.0							1985	6.8
										1990	8.2
SA-4		−26.0	−78.0	1.10	6.27	8.2	26.24	0.11	7.3	1940	6.5
		−24.0	−60.0							1949	6.7
		−12.0	−60.0							1958	7.2
		−14.0	−78.0							1963	7.4
										1994	8.2
SA-5		−26.0	−78.0	1.10	6.55	7.5	26.29	0.30	7.4	1936	7.0
		−24.0	−60.0							1946	7.2
		−35.0	−60.0							1950	7.4
		−35.0	−78.0							1962	6.9
										1977	6.9
										1983	7.2
										1991	7.9
KK-1	Kuriles-Kamchatka	42.0	146.0	1.10	6.75	8.7	25.69	0.24	7.1	1932	6.5
		44.0	151.0							1939	6.8
		51.0	140.0							1987	6.6
		49.0	135.0							1990	7.8
KK-2		44.0	151.0	1.10	6.39	7.5	25.61	0.17	7.3	1972	6.5
		47.0	156.0							1984	6.8
		53.0	145.0							1987	6.8
		51.0	149.0								
KK-3		47.0	156.0	1.10	5.76	8.0	25.67	0.18	7.0	1970	8.0
		49.0	160.0								
		55.0	149.0								

Table 1 (*continued*)

Region		Lat.	Long.	b'	a	M_{max}	log m_o	P_{10}	M_f	Year	M_{cum}
		53.0	145.0								
JP-2	Japan	33.0	135.0	1.10	6.37	7.8	26.21	0.03	7.5	1935	6.5
		36.5	145.0							1940	7.5
		39.0	145.0							1957	7.1
		46.0	132.0							1973	7.8
		42.0	125.0							1994	7.8
PH-6	Philippines	04.5	121.0	1.10	6.17	7.8	26.01	0.18	7.3	1935	6.5
		04.5	129.0							1940	7.2
		10.2	129.0							1972	6.9
		10.2	121.0							1984	7.8
IBM-1	Izu-Bonin Marianas	25.5	135.0	1.10	6.54	7.8	26.38	0.84	7.5	1940	7.0
		25.5	145.0							1961	7.0
		36.5	145.0							1956	7.3
		33.0	135.0							1970	7.3
										1978	7.9
										1990	6.9
IBM-2		25.5	140.0	1.10	5.72	7.2	25.35	0.57	7.0	1937	6.5
		25.5	146.0							1955	7.1
		20.0	146.0								
		20.0	140.0								
IBM-3		20.0	143.0	1.10	5.87	7.0	25.44	0.50	7.1	1931	6.7
		20.0	149.0							1962	7.0
		16.0	149.0							1979	7.0
		16.0	143.0								
IND-3	Indonesia	−03.0	104.0	1.10	5.98	7.2	25.61	0.08	7.0	1952	6.9
		−03.0	112.0							1957	7.4
		−10.0	112.0							1994	7.1
		−10.0	114.0								
IND-4		−04.0	112.0	1.10	6.11	7.2	25.74	0.54	7.2	1937	7.3
		−04.0	119.0							1953	6.7
		−10.0	119.0							1968	7.2
		−10.0	112.0							1987	6.8
IND-5		−04.0	119.0	1.10	6.57	8.0	26.48	0.53	7.3	1937	7.3
		−04.0	127.0							1952	7.0
		−10.0	127.0							1957	7.4
		−10.0	119.0							1968	7.2
										1987	6.5
										1994	7.2
TNG-1	Tonga	−14.0	−170.0	1.10	6.60	8.0	26.51	0.04	7.2	1941	7.1
		−14.0	175.0							1956	7.7
		−18.0	175.0							1974	6.9
		−18.0	−170.0							1984	6.5
										1994	8.0
TNG-2		−21.0	−170.0	1.10	6.67	7.5	26.41	0.36	7.3	1935	7.3
		−21.0	175.0							1948	7.2
		−18.0	175.0							1957	7.4
		−18.0	−170.0							1967	7.2
										1979	6.7
										1986	7.7
TNG-3		−21.0	−170.0	1.10	6.74	7.7	26.54	0.61	7.4	1932	7.8
		−21.0	175.0							1944	7.1
		−26.5	175.0							1954	6.8
		−26.5	−170.0							1959	7.4
										1973	7.6
										1986	7.5

criteria the seismogenic regions were defined as parts of the subduction zones having as much as possible the same properties of the above mentioned. Papazachos and Papadimitriou (1997) have showed that different zonation techniques do not significantly affect the results of the model. For this reason, they used a data set from Italy and an independent zonation published by Mulargia and Gasperini (1995) in order to examine the model dependence on zonation. The results obtained by the application of the model to this independent data set demonstrated the robustness of the model and of the procedure followed. This means that the precise zonation is necessary and ameliorates the application of the model, but it is not critical. The final distribution of the defined seismogenic regions is shown in Fig. 1, where the regions are depicted as polygons with their coordinates given in Table 1.

The depth below which the trend of the Benioff zone begins to differentiate from its shallow part varies somewhat, but in most cases is deeper than 200–300 km. Therefore, for each Benioff zone three groups of seismogenic regions were considered, corresponding to three depth ranges. The first group concerns the regions including earthquakes with depths varying between 60 and 200 km, the second group includes the regions with events of 201–400 km, while the third group includes the deep seismicity ($h > 400$ km).

The complete data sample was used in order to calculate the seismicity parameters a and b of the Gutenberg–Richter (1944) relation. Since the value of b parameter is important for all the estimations of the current work, the complete sample of data was used for each depth range and a single b value was determined for each depth range. We prefer the use of a single robust b value rather than a local estimate for each seismic region due to large errors introduced in b in the cases where a limited number of data is available. Moreover, since for each seismic region the a value was also estimated after the b value is fixed, small errors in b have a negligible effect on the moment rate estimation which 'integrates' the Gutenberg–Richter curve. The b-values obtained were equal to 1.1, 0.9 and 1.1 for the depth ranges 60–200, 200–400, and >400 km, respectively. These values are in quite good agreement with the results of Giardini (1988) who analyzed the frequency distribution of deep earthquakes ($h > 350$ km) and obtained regional b-values in the range $0.4 < b < 1.22$, with a worldwide average value $b = 0.87$. The seismicity parameters and the coordinates of each seismogenic region are given along with other information in Table 1.

3. Estimation of the model parameters

Papazachos and his colleagues (1997a) have used a large amount of data including all the available information of the large shallow earthquakes of the continental fracture system in order to estimate the parameters of the two empirical formulae (Eqs. (1) and (2)) expressing the regional time and magnitude predictable model. These parameters can be considered as globally acceptable since they have been derived from a global data set and are not based on limited information coming from only one seismogenic region or one seismic area. For this reason, the values of the parameters b, c, d, B, C, D were adopted as they have been originally defined for shallow events, while the parameters q and m are estimated for each subduction zone and depth range. In order to proceed in this estimation, events with $M \geq 6.5$ during the period 1930–1995 and $M \geq 7.0$ during the period 1897–1995 have been taken into account.

The seismic moment rate, m_o (in dyn cm yr^{-1}), is one of the most important parameters for the application of the model, since it expresses the tectonic loading exerted in the volume of each seismogenic region. For its determination, a procedure proposed by Molnar (1979) was applied. According to this procedure, the number of events with seismic moment equal or larger than M_o is given by the relation:

$$N(M_o) = GM_o^{-E} \tag{6}$$

where

$$G = 10^{a+(b'k/r)} \text{ and } E = \frac{b'}{r} \tag{7}$$

and a, b' are the constants of the Gutenberg–Richter (1944) relation normalized for one year, and r, k the parameters of the moment–magnitude relation:

$$\log M_o = rM + k \tag{8}$$

Table 2
The model parameters, q and m, along with their standard deviations (σ_q and σ_m), for the eleven areas and three depth ranges of the circum-Pacific subduction zones. The mean number of mainshocks per decade in each area, λ_{10}, and the expected number of such mainshocks, $\sum P_{10}$, according to the calculated model probabilities, are also given

Area	61 –200 km						201–400 km						> 400 km					
	q	σ_q	m	σ_m	λ_{10}	$\sum P_{10}$	q	σ_q	m	σ_m	λ_{10}	$\sum P_{10}$	q	σ_q	m	σ_m	λ_{10}	$\sum P_{10}$
South America	7.57	0.18	−6.17	0.29	5.78	3.85	7.77	0.27	−6.22	0.40	0.58	0.12	7.65	0.28	−6.04	0.46	2.47	1.08
Middle America	7.65	0.20	−6.19	0.32	2.59	3.70	–	–	–	–	–	–	–	–	–	–	–	–
North Pacific	7.67	0.28	−6.40	0.21	1.64	1.54	–	–	–	–	–	–	–	–	–	–	–	–
Kamchatka-Kuriles	7.59	0.19	−6.05	0.45	3.88	2.62	7.61	0.08	−5.95	0.32	0.83	0.99	7.54	0.55	−6.11	0.51	0.43	
Japan	7.63	0.36	−6.09	0.59	2.00	1.03	7.78	0.17	−6.48	0.12		1.19	7.67	0.13	−5.89	0.36	0.74	0.03
Izu Bonin - Marianas	7.57	0.28	−6.12	0.44	3.86	2.30	7.74	0.23	−6.21	0.36	1.00	0.39	7.58	0.18	−6.24	0.31	2.50	2.06
Philippines	7.63	0.23	−6.25	0.39	5.93	4.12	7.71	0.10	−6.08	0.14		0.07	7.80	0.25	−5.98	0.40	0.45	0.18
Indonesia	7.55	0.26	−6.12	0.39	5.33	4.45	7.43	0.08	−5.99	0.24	1.33	2.98	7.72	0.21	−6.34	0.23	2.07	1.15
Guinea	7.59	0.19	−6.17	0.36	4.83	2.90	7.43	0.19	−6.10	0.23		0.69	–	–	–	–	–	–
Solomon - Hebrides	7.62	0.25	−6.20	0.39	5.98	3.96	7.58	0.16	−6.11	0.28	1.67	1.28	–	–	–	–	–	–
Tonga - Kermadec	7.60	0.19	−6.09	0.45	3.88	3.53	7.69	0.26	−6.30	0.25	2.15	1.70	7.75	0.16	−6.23	0.32	2.48	1.21

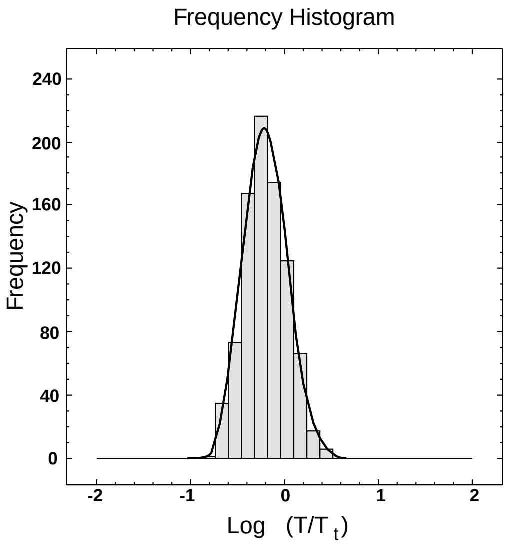

Fig. 2. Frequency distribution of logarithm of the ratio of the observed interevent times, T, to the theoretical interevent times, T_t, predicted from the time-predictable model, as this is determined for 98 seismic regions-depth ranges of all the subduction zones examined in the present study.

For the present case, it is taken $r = 1.44$ and $k = 16.56$ according to the relation proposed by McGarr (1977) for intermediate and deep earthquakes. The relation then gives the rate of seismic moment release:

$$m_o = \frac{G}{1-E} M_{o,max}^{1-E} \tag{9}$$

where $M_{o,max}$ is the seismic moment released by the maximum earthquake in the region with magnitude M_{max}.

The present method applies to mainshocks, that is, to the largest shocks of each group of earthquakes clustered in time and space. Since only the main shocks (in the broad sense) are needed, their pre-shocks (foreshocks in the broad sense) and post-shocks (aftershocks in the broad sense) are excluded from the data sample according to the formula:

$$t_p = 3 \text{ yr}, \qquad \log t_a = 0.06 + 0.13 M_p \tag{10}$$

proposed by Papazachos et al. (1997a), which gives the duration of the pre-shock, t_p, and post-shock, t_a, activity as a function of the magnitude of the preceding mainshock. Several techniques have been tested for "data declustering" and the one followed here was found the more suitable one. As far as the spatial window in which the declustering is done, the region's dimensions implicitly limit it, since relation (10) applies in each such region separately. This "declustered" data set is then used for the estimation of the parameter q and m in each subduction zone and for the three depth ranges described previously. The data sample used for this calculation consists of 894 sets (T, M_{min}, M_p, and M_f) and concerns 98 seismogenic regions. The values of parameter q and m of Eqs. (1) and (2), along with their standard deviations, are given in Table 2.

Using the values determined and Eq. (1), the theoretical interevent times, T_t, were estimated for each seismogenic region. Fig. 2 illustrates the frequency distribution of log (T/T_t) for the interevent times, T, of all 98 examined cases (regions-depth ranges-minimum magnitude) of all the subduction zones, together with the best-fit normal distribution which has an average value of $\mu = -0.10$ and a standard deviation of $\sigma = 0.24$. This standard deviation is usually attributed to the intrinsic limitations of the model as well as to the quality and quantity of input data and which varies from region to region (Scholz,

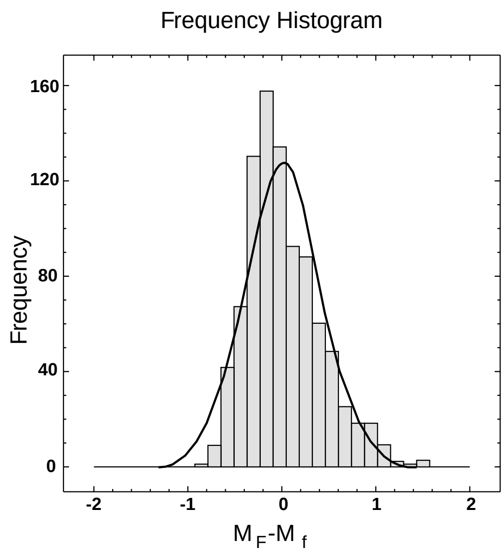

Fig. 3. Same as Fig. 2 for the magnitude difference between the observed, M_F, and predicted M_f, magnitude of the next mainshock for the same seismic regions-depth ranges. Both distributions exhibit a more or less Gaussian shape.

1990). The data quality mainly concerns magnitude estimation precision, since occurrence time is precisely known for each event.

Papazachos et al. (1997a) found a standard deviation equal to 0.28 for the seismogenic sources of the continental fracture system. It is interesting to note that Nishenko and Buland (1987) found a value equal to 0.21 for the corresponding intrinsic standard deviation for mainshocks in plate boundaries. To compare the observed and the theoretical (solid line) distributions, the Kolmogorov–Smirnov test was applied. It was found that the statistics, D_k, i.e. the largest absolute difference between the obtained and the theoretical cumulative relative frequencies, is 0.02 at 0.86 significance level, and the critical value of D_k at this level is 0.04. This means that the hypothesis of normal distribution of the quantity log (T/T_t) should be considered to be valid.

Fig. 3 shows the frequency distribution of the magnitude difference, $M_F - M_f$, between the observed magnitude, M_F, and the calculated magnitude, M_f, using relation (2) for all the seismogenic regions of the subduction zones. The best fit normal distribution with $\mu = 0.05$ and a standard deviation equal to $\sigma = 0.38$ is also shown. This value of σ is larger than the one found for the time predictable model, and it is attributed to the fact that in this case only magnitudes are involved in the estimations. The corresponding value found by Papazachos et al. (1997a) for the continental fracture system was equal to $\sigma = 0.36$.

This residual distributions of Figs. 2 and 3 demonstrate the very good applicability, especially for the time-predictable model (Eq. (1), Fig. 2) for deep earthquakes. This is a promising result, considering the different nature and geotectonic environment in which deep events occur. In the following, we examine the statistical reliability of this result using probability estimates derived after applying the time- and magnitude-predictable model.

4. Probability estimates

Since the earthquakes are known to exhibit long-term variations of activity (Ambraseys and Melville, 1982; Veneziano and Chouinard, 1989; Kagan and Jackson, 1991a) we need some quantitative rule that assigns a different weight to seismic events depending on the elapsed time since their occurrence. Probabilities must then be calculated given a gap time since the last event and the magnitude of the previous and future event. In order to proceed to the determination of model probabilities, the probability density function of the observed interevent time, T, to the calculated one, T_t, as this later is calculated by relation (1), must be known. Once this function is defined, earthquake repeat time estimates can be presented in terms of a conditional probability, which describes the likelihood of failure within a given time interval, $t + \Delta t$, provided that the event has not occurred during the time t. From several previous studies (Nishenko and Buland, 1987; Davis et al., 1989) as well as the fit shown in Fig. 2 it appears that the lognormal distribution of T/T_t is more suitable.

For the calculation of the model probabilities, the corresponding standard deviation is also needed (Papazachos and Papaioannou, 1993) and this quantity, σ_q, is given in Table 2 for each area. Similarly, Eq. (2) can be applied to estimate the magnitude of the expected mainshock in each seismogenic region since the value of the parameter m is given in Table 2 for each seismic area. A measure of the uncertainty in this

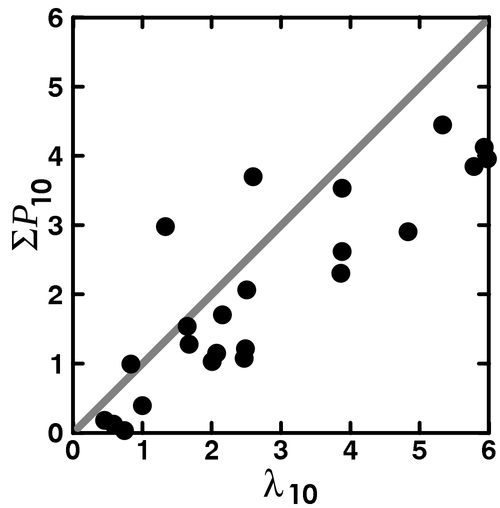

Fig. 4. Comparison between the sum of the probabilities for each decade of the present century, $\sum P_{10}$, determined from the time-predictable model for all seismic regions-depth ranges and the number of mainshocks, λ_{10}, which occurred in these seismic regions-depth ranges during each decade. A relatively good linear correlation is observed.

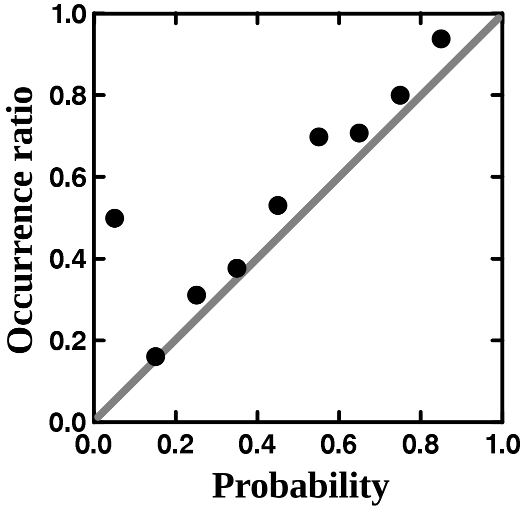

Fig. 5. Comparison between the probability predicted for each seismic region-depth range using the time-predictable model for each decade of the present century and the occurrence ratio, which is defined as the ratio of the number of cases (decades of the present century/seismic regions/depth ranges) where a deep earthquake occurred to the total number of examined cases. A very good linear correlation is observed. An exception is observed for the areas of very low probability (after a large mainshock) which indicates the relatively low efficiency of the declustering procedure (removal or pre and post-shocks) determined from shallow events for areas of deep seismicity.

estimation is the corresponding standard deviation, σ_m, which is also given for each area in Table 2. The probabilities of occurrence of the next large ($M \geq 7.0$) mainshock during the next 10 yr in each seismogenic region, as well as its expected magnitude, can then be estimated and are presented in Table 1 for each seismic region and depth range.

In order to check the internal consistency of the model two tests were performed. In the first test, the model probabilities for the occurrence of mainshocks larger than a certain magnitude threshold in a certain area during the next 10 yr, $\sum P_{10}$, with the mean number of such mainshocks per decade, λ_{10}, was compared. In principle, these two quantities should be more or less equal. In the cases where $\sum P_{10} > \lambda_{10}$ or $\sum P_{10} < \lambda_{10}$, a relatively strong or quiet seismic activity is expected for the examined period (10 yr), respectively.

In the present paper, this test was made for mainshocks with $M_s \geq 6.5$ which occurred in each one of the subduction zones and for the three depth ranges for all the decades of the present century. The calculated values of λ_{10} and $\sum P_{10}$ are also given in Table 2 and the corresponding plot is shown in Fig. 4. A good correlation between these two quantities is observed, indicative of the reliability of the method.

In the second test a post-verification of the predictive ability of Eq. (1) was performed. For each decade of the present century, the probability for all seismic regions and depth ranges was estimated. For all cases showing a similar probability range, e.g. 10–20% the occurrence ratio was estimated, that is, the ratio of cases when an earthquake occurred to the total number of examined cases. If the model has a good predictive ability, these quantities should be equal. The comparison of the occurrence ratio with model probability is shown in Fig. 5. An excellent correlation is observed between the two quantities, indicating that the model appropriately describes the time behavior

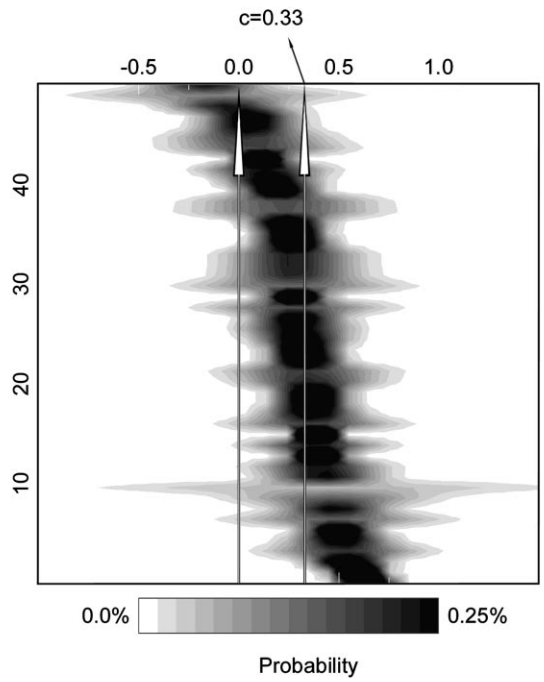

Fig. 6. Grey-scale plot of the probability density distribution for the 52 cases (seismic regions-depth ranges) examined in the present study. The probabilities are shown for each c value (horizontal axis) and all cases (vertical axis), after sorting the examined cases for their c-values. Dark colored areas denote high probability c-values. The average c ($=0.33$) and $c=0$ levels are also shown. A clear distribution of positive c value is observed for almost all cases.

of seismicity. The only exception is the case of very low probability (0–10%) where a very high occurrence ratio (~50%) is observed. This observation is a clear indication of inefficient declustering: after a mainshock, the model probabilities are very low (0–10%) but a large number of aftershocks of this main shock still occur. These aftershocks are removed during the declustering procedure (Eq. (10)). The large probabilities seen in Fig. 4 for this low probability interval (0–10%) indicate that the declustering procedure followed in the present work is probably not completely removing these aftershocks. The large probabilities observed in Fig. 2 suggest that the aftershock activity for deep events has a larger duration than for shallow events.

5. Validation of the time- and magnitude-predictable model

All the processing previously described focused on testing the time- and magnitude predictable model for shallow events 'as it is' on deep events, hence no optimization is involved. The essence of the time- and magnitude- predictable models is the incorporation of terms cM_p and CM_p in Eqs. (1) and (2), respectively. Hence, in order to prove the efficiency of this model, the statistical significance of these terms has to be demonstrated. For this reason, we decided to study these terms separately, even if they are estimated by only a limited number of data concerning only one seismogenic region. Since for each seismogenic region both terms including M_{min} and m_o are constant, relations (1) and (2) are of the form:

$$\log T_t = cM_p + q' \quad (11)$$

$$M_f = CM_p + m' \quad (12)$$

where q' and m' depend on M_{min}, m_o and the seismogenic region studied. For each region and depth range for which data were available, several M_{min}-values were selected (depending on the available data). The values of c and C, as well as their errors were estimated for each of the 52 region-depth range-M_{min} combinations. The results are shown in Fig. 6 where the probability density distribution is presented for all the obtained c-values. In this figure, the probability density function is presented for the c-values (horizontal axis) which are sorted and presented for the 52 cases (for which more than five data sets for the same M_{min} are available) along the vertical axis. Dark colored areas denote c-values of high probability while light colored areas have low probabilities. The average value of c is equal to 0.33 (shown in Fig. 6), which is equal to the value found for shallow events. Although for some cases the c-values show a large variance (broad distribution of probabilities), the large majority of cases show positive c-values. A strict estimation of the statistical significance of the c-values by examining each case separately shows that only for 35% of the examined cases can it be proved that $c > 0$ with a 90% confidence. This is probably due to the small magnitude range that the data cover for each seismic group. However, the statistical tests for each case separately do not take into account the fact that we observe a similar behavior for almost all cases. Therefore, a different methodology has been introduced, where it was tested if the model has a global applicability, even if the time intervals vary on the average among different cases (different regions, seismicity, etc.). The results shown in Fig. 6 demonstrate that the positive linear dependence of $\log T - M_p$ should not be considered and evaluated as a local but a global phenomenon.

In order to further demonstrate this global behavior between the interevent times and the magnitude of the preceding event, we follow Papazachos and Papadimitriou (1997) and assume that a single constant, $\bar{c}$, applies for all zones, that is:

$$\log T_k^{(i)} = \bar{c}M_{p_k} + \sum_{j=1}^{n} \delta_{ij} a_j = \bar{c}M_{p_k} + a_i \quad (13)$$

$$k = 1, \ldots, m$$

where the $T_k^{(i)}$ and M_{p_k} belong to the i group of data (specific seismic region, depth range, M_{min}), a_j is the constant which corresponds to each case j, n is the number of the available groups of data (cases) and m is the total number of the available data ($T_k^{(i)} - M_{p_k}$ pairs). It is clear that Eq. (13) considers the complete data set. The kth datum, $T_k^{(i)}$, is now controlled by two different factors, namely M_{p_k} and the group i (seismic region–depth–M_{min}) where it belongs. Eq. (13) forms the following linear system:

$$\begin{bmatrix} \log T_1^{(1)} \\ \log T_2^{(1)} \\ \vdots \\ \log T_k^{(2)} \\ \vdots \\ \log T_m^{(n)} \end{bmatrix} = \begin{bmatrix} M_{p_1} & 1 & 0 & \cdots & 0 \\ M_{p_2} & 1 & 0 & \cdots & 0 \\ \vdots & \vdots & \vdots & \ddots & \vdots \\ M_{p_k} & 0 & 1 & \cdots & 0 \\ \vdots & \vdots & \vdots & \ddots & \vdots \\ M_{p_m} & 0 & 0 & \cdots & 1 \end{bmatrix} \begin{bmatrix} c \\ a_1 \\ a_2 \\ \vdots \\ \vdots \\ a_n \end{bmatrix} \quad (14)$$

or using a matrix notation:

$$T = Aa \quad (15)$$

In our case, 282 data sets (T, $M_{\min}$, M_p, M_f) were available for the linear system (15) which was solved using standard least squares' solution for the determination of $\bar{c}$ and the $n = 51$ constants a_i. The final c value was $\bar{c} = 0.31 \pm 0.03$. The generalized linear correlation coefficient of Eq. (13) was $r = 0.63$ and the corresponding standard error was equal to $\sigma_{\log T} = 0.19$. It should be noted that this is a generalized (for 52 parameters estimated in Eq. (14)) and not a simple 2-parameter linear correlation coefficient, hence, it is much more reliable than the individual ones estimated for each one case. It is interesting to notice that the value of c estimated for shallow events is $c = 0.33$, which is practically equal to the value determined here.

The error reported for $\bar{c}$ is a marginal error; i.e. is valid only if the values for a_i are correct. The true confidence area for $\bar{c}$ is described by the ellipsoid:

$$\Delta\chi^2 = \mathbf{da}^{\mathrm{T}}\mathbf{C_a}^{-1}\mathbf{da} \quad (16)$$

where $\Delta\chi^2$ is the allowed increase of the misfit, χ^2, for $n + 1$ degrees of freedom given the perturbation vector **da** and the covariance matrix of the solution of Eq. (15), $\mathbf{C_a}$. Following Papazachos and Papadimitriou (1997) we can estimate the minimum possible $\bar{c}$ value in the 95% confidence ellipsoid which was found equal to 0.16. We observe that for even these strict confidence limits for $\bar{c}$, its value is always positive. A similar situation has been shown to hold for shallow events (Papazachos and Papadimitriou, 1997).

A similar equation can be assumed for the magnitude-predictable model:

$$M_{a_i} = \bar{C}M_{p_i} + \sum_{j=1}^{n} \delta_{ij}A_j = \bar{C}M_{p_i} + A_i \quad (17)$$

The parameters of the magnitude-predictable model can be estimated using a similar procedure. The average value determined was $\bar{C} = -0.13 + 0.047$, with standard error of $\sigma_{M_a} = 0.43$ and a generalized linear correlation coefficient $r = 0.56$. The obtained value, $\bar{C}$, is quite smaller than the value determined for shallow events ($= -0.28$). This can be also identified in Fig. 2 where the distribution of $M_a^{\mathrm{obs}} - M_a^{\mathrm{calc}}$ show a clear asymmetry compared to the normal distribution, due to the very different C value obtained here from the value used in Fig. 3. Moreover, in the 95% error ellipsoid, a very small number of solutions have a positive C value and the maximum possible C value is 0.06. Therefore, we conclude that the magnitude-predictable model is not as robust as the time-predictable model at least for deep events, also shown by the smaller linear correlation coefficient, similar to the observation made for shallow events (Papazachos et al., 1997a,b).

Combination of Eqs. (13) and (17) leads to an equation, which resembles the slip-predictable model:

$$\log T_i = \bar{E}M_{a_i} + \sum_{j=1}^{n} \delta_{ij}D_j = \bar{E}M_{a_i} + D_i \quad (18)$$

Following the previously described procedure for the estimation of $\bar{E}$ leads to a value of $\bar{E} = -0.19$ with a low linear correlation coefficient ($r = 0.44$). However, the essence of the slip-predictable model is that $\bar{E}$ is positive and not negative as we found here, since large interevent times, T, should lead to large earthquakes, M_a, if this model applies. The estimated Eq. (18) does not express any physical law, but it is a simple mathematical result of the combinations of the time- (Eq. (13)) and the magnitude (Eq. (17)) predictable models. Therefore, the slip-predictable model (large events follow large interevent times) should be rejected for deep events, similarly to the observation made for shallow ones.

6. Discussion

Since the introduction of the "time-predictable model" (including Bufe et al., 1977) and the "slip predictable model" (Shimazaki and Nakata, 1980) considerable research work has been performed, towards the verification of the applicability of these models for specific areas or on a global scale. Several authors have made important contributions and suggestions including Papazachos (1989, 1992), which have generally favored such models, especially the time-predictable model. Laboratory experiments on stick–slip behavior on pre-existing faults also favor the model (Sykes, 1983). On the other hand, various authors have questioned the applicability of such models. Davis et al. (1989) have contradicted to any model taking account the elapsed time since the last event in a specific region and suggested that clustering of events for all magnitudes should be considered as a probable scenario. This opinion implies aperiodicity values larger than 1, where aperiodicity is defined as $c_v = \sigma/\bar{T}$, the ratio of the standard deviation, σ, to the mean repeat time, $\bar{T}$ (Kagan and Jackson, 1991a,b). Notice that $c_v = 0$ and $c_v = 1$ correspond to periodic and Poissonian behavior, respectively. Sornette and Knopoff (1997) proved that any distribution that falls off at large time intervals at a faster rate than an exponential, such as periodic, quasiperiodic, uniform, and semi-Gaussian distributions, and the Weibull distribution with $m > 1$, has the property 'the longer it has been since the last earthquake, the shorter the expected time until the next'. The later is the principle of the regional time and magnitude predictable model and for this reason the temporal behavior of the mainshocks used for its application, is discussed here. Mulargia and Gasperini (1995) tested the applicability of the time- and slip-predictable earthquake recurrence models to Italian seismicity through a strict statistical procedure. They suggested that such models offered a satisfactory fit (90% confidence) in just two regions and one region for the time- and slip-predictable models, respectively, out of 19 globally analyzed. However, in each of their samples, where this test was applied, the uncertainties of the earthquake size (errors in the magnitude, seismic moment, coseismic slip) are comparable with the range of this size (difference between maximum and minimum size).

Papazachos and Papadimitriou (1997) questioned these results since they showed that we could not rely on statistical tests for a single seismogenic region, mainly due to errors in the magnitude estimation and the small magnitude range spanned by available data. Moreover, they showed that an alternative procedure can be applied demonstrating the high statistical significance (>95%) of the global applicability of the time- and magnitude- predictable models. As far as the quasi-periodical behavior of the mainshocks is concerned, Papazachos et al. (1997a) estimated a mean c_v — value equal to 0.56 for a global data set, which corresponds to a quasi-periodical time behavior. Nishenko and Buland (1987) also found that $M = 7.0$ events behave quasi-periodically with an intrinsic (lognormal) aperiodicity of 0.21. Goes and Ward (1994) by examining recurrence statistics for a fault model in San Andreas, pointed out that there is a clear trend of decreasing aperiodicity with increasing event magnitude. Only the largest events (M at least 7) display quasi-periodic behavior, while toward lower magnitudes, M 6–6.5, clustering becomes the dominant mode of recurrence, as these events are often fore- or aftershocks.

The time-, slip- and magnitude-predictable models have attracted the interest of many scientists who discussed the aspects related (definition of the seismogenic regions, temporal behavior of the main shocks, moment rate, probability estimation) and agree or disagree with some of them or reject the model. It has been shown that the accurate definition of the seismogenic regions, which include not only the major fault but other secondary faults as well, is necessary for a more reliable estimation of the basic parameters of relations (1) and (2), but it is not critical for the model application. From an inspection on the temporal distribution of the mainshocks, it was derived that they behave quasi-periodically. The moment rate is almost the same if either only the large events are considered or the methodology followed here. This provides a tool to obtain such value even in the cases where no large earthquake is included in the complete data sample and to take into account the maximum earthquake ever occurred in the region. Moreover, statistical tests have shown that the probability estimates are close to the reality when they compared with the rate of occurrence and against time independent models. All the above are explicitly discussed in detail in Papazachos et al. (1997a) and Papazachos and Papadimitriou (1997).

In the present work, we proceed one step further by examining the time- and magnitude-predictable models globally defined for shallow events, on a completely independent data set that includes deep events. The very good applicability of each of these models and especially the time-predictable model, on such a very different data set (deep events instead of shallow), suggests that this time-magnitude dependence on the magnitude of the preceding event is a general characteristic of all earthquakes, at least for large mainshocks. Further analysis, following Papazachos and Papadimitriou (1997), demonstrated the global applicability of the time-predictable model for deep events although the magnitude-predictable model seems to be less robust.

The results of the present study indicate that even if prediction of a specific earthquake is not feasible, time-dependent earthquake prediction may still be possible, if we understand by 'prediction' a statement of earthquake probability in any time–space–magnitude and possibly focal mechanism window (Vere-Jones, 1978; Brillinger, 1982a,b; Molchan and Kagan, 1992; Nishenko and Sykes, 1993). The prediction probability, called earthquake potential by Wallace et al. (1984), should be defined in such cases as a conditional rate of earthquake occurrence, conditioned on the time, space and magnitude distribution of past earthquakes. If we adopt such a probabilistic point of view, we believe that the time - dependent seismicity model examined here for deep events provides a useful tool for the improvement of seismic hazard estimates.

Acknowledgements

The authors would like to express their sincere appreciation to Prof. B.C. Papazachos for his encouragement and fruitful discussions throughout the implementation of the present study. Gratitude is extended to Prof. Carl Kisslinger and two anonymous reviewers for their comments that considerably helped in the manuscript improvement. This paper is Department of Geophysics contribution number 547.

References

Abe, K., 1981. Magnitudes of large shallow earthquakes from 1904 to 1980. Phys. Earth Planet. Inter. 27, 72–92.

Abe, K., Kanamori, H., 1980. Magnitudes of great shallow earthquakes from 1953 to 1977. Tectonophysics 62, 191–203.

Ambraseys, N.N., Melville, C.P., 1982. A History of Persian Earthquakes. Cambridge University Press, New York, p. 1982.

Brillinger, D.R., 1982a. Some bounds for seismic risk. Bull. Seismol. Soc. Am. 72, 1403–1410.

Brillinger, D.R., 1982b. Seismic risk assessment: some statistical results. Earthquake Predict. Res. 1, 183–195.

Bufe, C.G., Harsch, P.W., Burford, R.O., 1977. Steady-state seismic slip: a precise recurrence model. Geophys. Res. Lett. 4, 91–94.

Davis, P.M., Jackson, D.D., Kagan, Y.Y., 1989. The longer it has been since the last earthquake, the longer the expected time till the next?. Bull. Seismol. Soc. Am. 79, 1439–1456.

Giardini, D., 1988. Frequency distribution and quantification of deep earthquakes. J. Geophys. Res. 93, 2095–2105.

Goes, S.D.B., Ward, S.N., 1994. Synthetic seismicity model for the San Andreas Fault. Ann. Geofis. 37, 1495–1513.

Gutenberg, B., Richter, C.F., 1944. Frequency of earthquakes in California. Bull. Seismol. Soc. Am. 34, 185–188.

Gutenberg, B., Richter, C.F., 1954. Seismicity of the Earth and Associated Phenomena. Princeton University, Princeton, NJ, 310 pp.

Hanks, T.C., Kanamori, H., 1979. A moment magnitude scale. J. Geophys. Res. 84, 2348–2350.

Heaton, T., Tajima, F., Mori, A., 1986. Estimating ground motions using recorded accelerograms. Surv. Geophys. 8, 25–83.

Kagan, Y.Y., Jackson, D.D., 1991a. Long-term earthquake clustering. Geophys. J. Int. 104, 117–133.

Kagan, Y.Y., Jackson, D.D., 1991b. Seismic gap hypothesis: ten years after. J. Geophys. Res. 96, 21419–21431.

Kanamori, H., 1977. The energy release in great earthquakes. J. Geophys. Res. 82, 2981–2987.

Karakaisis, G.F., 1994. Long-term earthquake prediction along the North and East Anatolian Fault Zones based on the time and magnitude predictable model. Geophys. J. Int. 116, 198–204.

Kostrov, B.V., Das, S., 1988. Principles of Earthquake Source Mechanics. Cambridge University, New York 286 pp.

McGarr, A., 1977. Seismic moments of earthquakes beneath island arcs, phase changes and subduction velocities. J. Geophys. Res. 82, 256–264.

Molchan, G.M., Kagan, Y.Y., 1992. Earthquake prediction and its optimization. J. Geophys. Res. 97, 4823–4838.

Molnar, P., 1979. Earthquake recurrence intervals and plate tectonics. Bull. Seismol. Soc. Am. 69, 115–133.

Mulargia, F., Gasperini, P., 1995. Evaluation of the applicability of the time- and slip-predictable recurrence models to Italian seismicity. Geophys. J. Int. 120, 453–473.

Nishenko, S.P., Buland, R., 1987. A generic recurrence interval distribution for earthquake forecasting. Bull. Seismol. Soc. Am. 77, 1382–1399.

Nishenko, S.P., Sykes, L.R., 1993. Comment on "Seismic gap hypothesis: ten years after", by Y.Y. Kagan and D.D. Jackson. J. Geophys. Res. 98, 9909–9916.

Noguchi, S., Abe, K., 1977. Earthquake source mechanism and M_s–m_B relation. J. Seismol. Soc. Jpn 30, 487–507.

Panagiotopoulos, D.G., 1995. Long term earthquake prediction in Central America and Caribbean sea based on the time and magnitude predictable model. Bull. Seismol. Soc. Am. 85, 1190–1201.

Papadimitriou, E.E., 1994. Long term prediction of large shallow mainshocks along the Tonga–Kermadec–New Zealand seismic zone based on a time and magnitude predictable model. Tectonophysics 235, 347–360.

Papadimitriou, E.E., Papazachos, B.C., 1994. Time dependent seismicity in the Indonesian region. J. Geophys. Res. 99, 15387–15398.

Papazachos, B.C., 1989. A time predictable model for earthquakes in Greece. Bull. Seismol. Soc. Am. 79, 77–84.

Papazachos, B.C., 1992. A time and magnitude predictable model for generation of shallow earthquakes in the Aegean area. Pure Appl. Geophys. 138, 287–308.

Papazachos, B.C., Papaioannou, Ch.A., 1993. Long term earthquake prediction in the Aegean area based on a time and magnitude predictable model. Pure Appl. Geophys. 140, 593–612.

Papazachos, B.C., Papadimitriou, E.E., Karakaisis, G.F., 1994a. Time dependent seismicity in the zones of the continental fracture system. Proceedings of the XXIV General Assembly of ESC, Athens, 19–24 September 1994, 1099–1107.

Papazachos, B.C., Karakaisis, G.F., Papadimitriou, E.E., Papaioannou, Ch.A., Tsapanos, T.M., 1994b. Time dependent seismicity in the Alpine–Himalayan seismic belt. Bull. Hellenic Geol. Soc. XXX (5), 123–136.

Papazachos, B.C., Papadimitriou, E.E., Karakaisis, G.F., Panagiotopoulos, D.G., 1997a. Long-term earthquake prediction in the circum-Pacific convergent belt. Pure Appl. Geophys. 149, 173–217.

Papazachos, B.C., Papadimitriou, E.E., Karakaisis, G.F., Papaioannou, Ch.A., 1997b. The regional time and magnitude predictable model and its application to the Alpine–Himalayan belt. Tectonophysics 271, 295–323.

Papazachos, B.C., Kiratzi, A.A., Karakostas, B.G., 1997c. Measures of earthquake size used in Greece. Bull. Seismol. Soc. Am. 87, 474–483.

Papazachos, C.B., Papadimitriou, E.E., 1997. Evaluation of the global applicability of the regional time- and magnitude-predictable seismicity model. Bull. Seismol. Soc. Am. 87, 799–808.

Richter, C.F., 1958. Elementary Seismology. W. H. Freeman, San Francisco.

Rothe, J.P., 1969. The seismicity of the Earth 1953–1965. UNESCO.

Scholz, C.H., 1990. The mechanics of Earthquakes and Faulting. Cambridge University Press, New York, 349 pp.

Shimazaki, K., Nakata, T., 1980. Time-predictable recurrence model for large earthquakes. Geophys. Res. Lett. 7, 279–282.

Sornette, D., Knopoff, L., 1997. The paradox of the expected time until the next earthquake. Bull. Seismol. Soc. Am. 87, 789–798.

Sykes, L.R., 1983. Predicting great earthquakes. In: Kanamori, H., Boschi, E. (Eds.), Earthquakes, Theory and Interpretation. Elsevier, North-Holland, pp. 398–435.

Sykes, L.R., Quittmeyer, R.C., 1981. Repeat times of great earthquakes along simple plate boundaries. In: Simpson, D.W., Richards, R.G. (Eds.), Earthquake Prediction, An International Review. Maurice Ewing Series, vol. 4. American Geophysics Union, pp. 217–247.

Veneziano, D., Chouinard, L., 1989. Combination of seismic-source and historic estimates of earthquake hazard. Ann. N. Y. Acad. Sci. 558, 148–161.

Vere-Jones, D., 1978. Earthquake prediction — a statistician's view. J. Phys. Earth 26, 129–146.

Wallace, R.E., Davis, J.F., McNally, K.C., 1984. Terms for expressing earthquake potential, prediction and probability. Bull. Seismol. Soc. Am. 74, 1819–1825.